Supplementary Information

Effect of oxygen species, catalyst structure and their performance to methane activation over Pd-Pt catalyst

Haojie Geng[1,2,], Zhongqing Yang[2], Zhuwan Li[1], Siyu Yu[1], Jinshuai Wang[1], Li Zhang[2,#]*

1. *School of Chemistry and Chemical Engineering, Southwest University, Chongqing 400715, China*
2. *School of Energy and Power Engineering, Chongqing University, Chongqing 400030, China*

S1. Reactivity of methane oxidation over monometallic sample

Figure S1 shows the calculation for first order rate coefficient of monometallic Pd and Pt sample in the manuscript. Methane pressure is positive to the reaction over both Pd and Pt monometallic sample. We see in **Figure S1** that high methane pressure contributes to high turnover rate of methane. Oxygen pressure is important to the reaction because the oxygen coverage and oxidability significantly affect the reaction region and rate-determining step. Methane pressure do not affect the catalyst structure, and in order to understand the kinetics, methane effect should be removed[1-3].

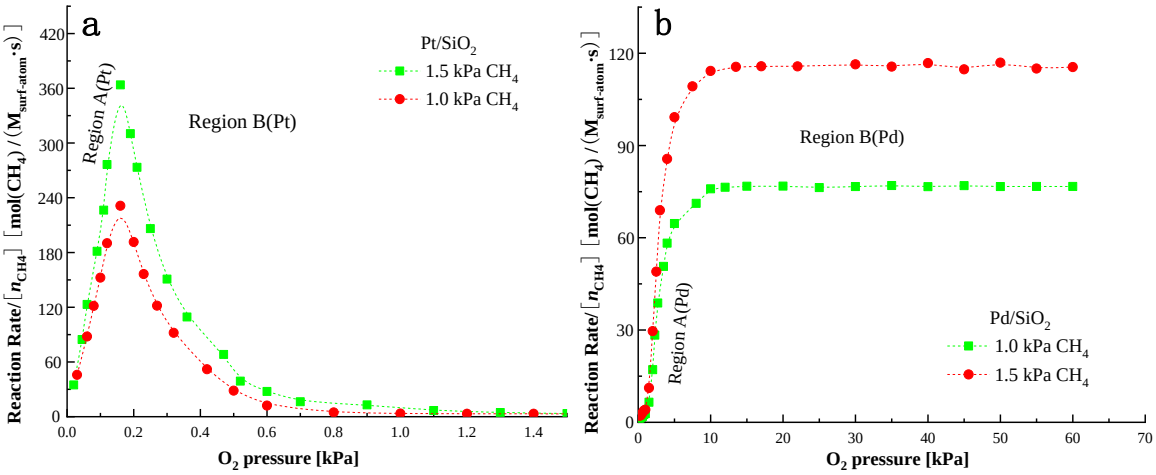

Figure S1. Reactivity of methane oxidation as a function of O_2 pressure over monometallic Pt (a) in low oxygen pressure, and monometallic Pd (b) in high oxygen pressure (1.0 kPa and 1.5 kPa CH_4, 100 mL/min total flow rate, N_2 balance, 300°C)

S2. Reactivity of methane oxidation over bimetallic sample

Corresponding author:
* Name: Haojie Geng, PhD, Lecturer, Email: hjgeng@swu.edu.cn;
# Name: Li Zhang, PhD, Professor, Email: lizhang_cqu@163.com;

Figure S2 shows the calculation for first order rate coefficient of bimetallic 1Pt1Pd and 1Pt2Pd sample in the manuscript. Catalytic consequences of Pt and Pd are separated via oxygen pressure at around 1 kPa. Methane pressure is positive to the reaction rate.

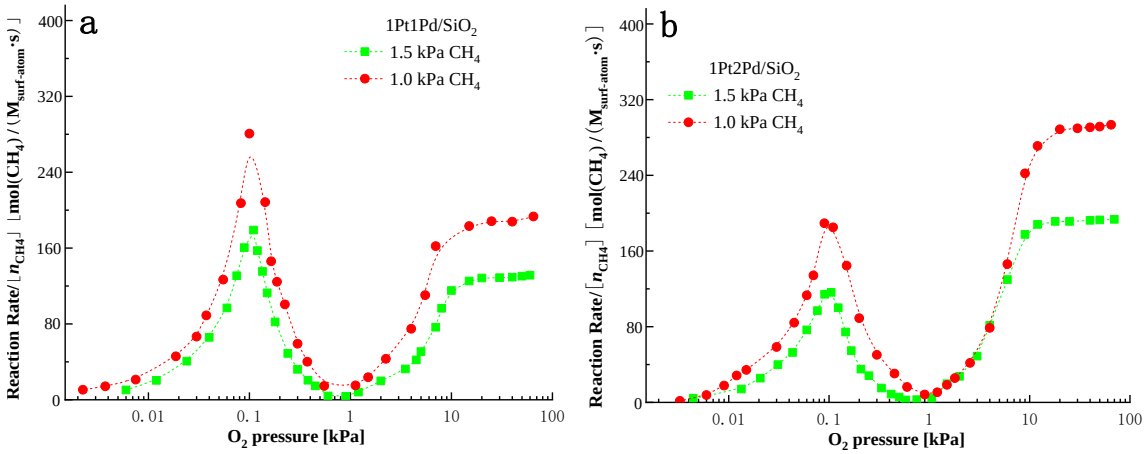

Figure S2. Reactivity of methane oxidation as a function of O_2 pressure over bimetallic 1Pt1Pd (a) and 1Pt2Pd (b) in a wide oxygen range (1.0 kPa and 1.5 kPa CH_4, 100 mL/min total flow rate, N_2 balance, 300℃)

S3. Average particle diameter calculated by hemisphere model

The average particle diameter mentioned above is calculated by arithmetic mean value from randomly selected particles. We use chemisorption data and hemisphere model to calculate the average particle size for comparison. The chemisorption at room temperature measures surface atoms on particle surface. All the atoms that are loaded on support surface can be calculated. Employing hemisphere model to calculate particle diameter requires that the catalyst can be regarded as a sphere to calculate the diameter. Some published report has used sphere model to evaluate the average diameter of monometallic Pd catalyst supported by alumina[4, 5], herein we expand its usage to Pd-Pt bimetallic samples. **Figure S3** shows the hemisphere model of Pd-Pt bimetallic and monometallic catalyst.

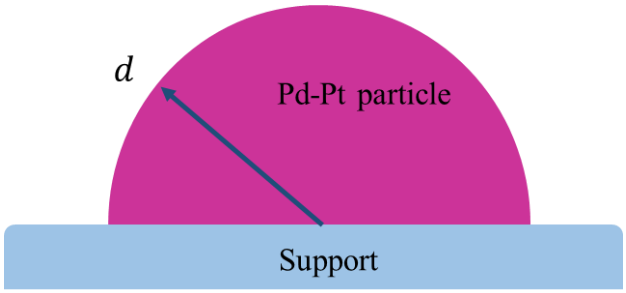

Figure S3. Hemisphere model of Pd-Pt bimetallic and monometallic catalyst

For all the particles, whether monometallic or bimetallic Pd-Pt particles, we define its average diameter as *d*. The surface area of each catalyst particle is:

$$S = 2\pi\left(\frac{d}{2}\right)^2 \quad (1)$$

S represents surface area of each particle. Then we could calculate surface atoms of each particle ($T_{surf,single}$) by using surface atoms concentration:

$$T_{surf,single} = {S \cdot k_{surf}}/{N_A} \quad (2)$$

N_A means Avogadro number, k_{surf} means surface atoms concentration. Herein, the surface atom concentration of Pd and Pt is $1.27 \times 10^{19}\ m^{-2}$ and $1.25 \times 10^{19}\ m^{-2}$, respectively, that is to say the two parameters are nearly the same. Therefore, in equation (2), k_{surf} choose $1.26 \times 10^{19}\ m^{-2}$ for bimetallic samples to do the calculation. Chemisorption result has measured total surface atoms of all the catalyst particles, thus we could obtain the total particle number on support surface:

$$N = \frac{n_{surf,total}}{{S \cdot k_{surf}}/{N_A}} \quad (3)$$

N means total particle number, $n_{surf,total}$ means all the surface atoms. Chemisorption experiment use oxygen as the probe molecule that can absorb on Pd or Pt species in the form of one to one. Pd and Pt species distribution on alloy surface does not affect the result measured from chemisorption.

Next, we establish the equation by using the equality of volume to calculate the average diameter. The total particle number has been calculated, thus employing the hemisphere model can write the total volume:

$$V = \frac{2}{3} \cdot \pi \cdot \left(\frac{d}{2}\right)^3 \cdot N \quad (4)$$

In the meantime, we know the loading percentage of Pd and Pt species, therefore we can calculate the volume by density:

$$V = \frac{n_{Pt,total} M_{Pt}}{\rho_{Pt}} + \frac{n_{Pd,total} M_{Pd}}{\rho_{Pd}} \quad (5)$$

If the sample is monometallic Pd or Pt catalyst, cancel the useless part in equation (5). $n_{Pt,total}$ and $n_{Pd,total}$ are molar mass for Pt and Pd, M_{Pt} and M_{Pd} are atomic weight of Pt and Pd, ρ_{Pt} and ρ_{Pd} are the density of bulk Pt and Pd. Combining with the equation (4) and (5), the average diameter (*d*) can be obtained.

S4. Lattice spacing, free energy of Pd and Pt species

Table S1 shows the parameters of lattice spacing, free energy of Pd and Pt species. It can be seen that oxidized Pd species has the lowest free energy in alloy catalyst[6, 7]. Compared with the surface free energy, oxidized Pd species still has the lowest value.

Generally, there is a migration force between two metal species in the process of crystal formation, which is caused by thermodynamic instability in alloy particle. Compared with Pd (100) and Pt (100) plane, surface free energy of Pt species is 2.48 J/m^2, which is higher than that of Pd species of 1.90 J/m^2. After oxidation, surface free energy of oxidized Pd further decreases to 0.53 J/m^2. Therefore, to maintain the stability of Pt-Pd binary metal system, Pd species will migrate to the surface as PdO, to reduce surface free energy of bimetal catalyst particle.[8, 9]

Table S1 Lattice spacing, surface free energy and bulk free energy for Pd and Pt species

Reduced Sample			**Oxidized Sample**				
Lattice fringe	Pt (111) 2.265 Å	**Bulk free energy**	PtO 7.73 kJ/mol	**Surface free energy**	Pt (100) 2.48 J/m^2		
	Pd (111) 2.246 Å		PtO_2 28.09 kJ/mol		Pd (100) 1.90 J/m^2		
	Pt-Pd (111) 2.25 Å		PdO -36.3 kJ/mol		PdO (100) 0.53 J/m^2		

S5. Representative image for Pd-Pt core-shell structure

In **Figure S4**, we select 3 representative core-shell structural particles, which shows a bright inner core (red circle) and outer shell (green circle). The brightness in the image, represents a higher atomic number (Pt species) in alloy particle. Therefore, Pt-Pd core-shell structural particles is displayed in these images. However, it should be point out that, not all Pd-Pt particles are core-shell structural particles. The formation of core shell structure needs a procedure of oxygen titration[10, 11].

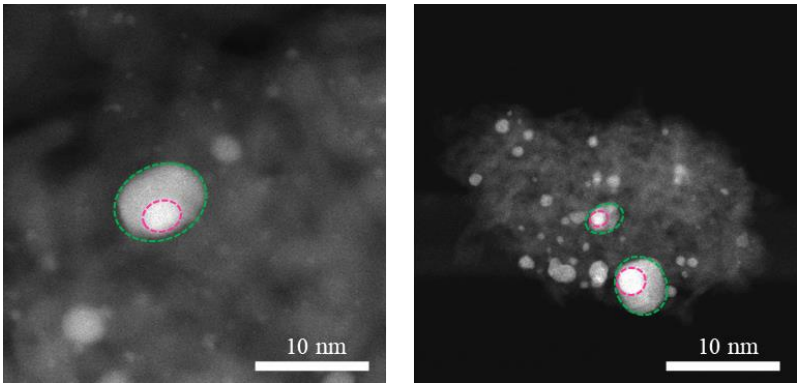

Figure S4. HAADF-STEM image for several representative core-shell structural Pd-Pt particles

Reference

[1] H. Geng, L. Zhang, Z. Yang, Y. Yan, J. Ran, Effect of Pd/Pt ratio on the reactivity of methane catalytic combustion in bimetallic Pd-Pt catalyst, International Journal of Hydrogen Energy, 43 (2018) 11069-11078.

[2] Y. Pang, Y. Dou, A. Zhong, W. Jiang, L. Gu, X. Feng, W. Ji, C. Au, Nanostructured Ru-Co@SiO_2: Highly efficient yet durable for CO_2 reforming of methane with a desirable H-2/CO ratio, Applied Catalysis a-General, 555 (2018) 27-35.

[3] Z. Xie, B. Yan, S. Kattel, J.H. Lee, S. Yao, Q. Wu, N. Rui, E. Gomez, Z. Liu, W. Xu, L. Zhang, J.G. Chen, Dry reforming of methane over CeO_2-supported Pt-Co catalysts with enhanced activity, Applied Catalysis B-Environmental, 236 (2018) 280-293.

[4] M. Cargnello, J.J. Delgado Jaen, J.C. Hernandez Garrido, K. Bakhmutsky, T. Montini, J.J. Calvino Gamez, R.J. Gorte, P. Fornasiero, Exceptional activity for methane combustion over modular Pd@CeO_2 subunits on functionalized Al_2O_3, Science, 337 (2012) 713-717.

[5] N.M. Martin, J. Nilsson, M. Skoglundh, E.C. Adams, X. Wang, P. Velin, G. Smedler, A. Raj, D. Thompsett, H.H. Brongersma, T. Grehl, G. Agostini, O. Mathon, S. Carlson, K. Noren, F.J. Martinez-Casado, Z. Matej, O. Balmes, P. Carlsson, Characterization of surface structure and oxidation/reduction behavior of Pd-Pt/Al_2O_3 model catalysts, Journal of Physical Chemistry C, 120 (2016) 28009-28020.

[6] A.M. Abdel-Mageed, K. Wiese, M. Parlinska-Wojtan, J. Rabeah, A. Brueckner, R.J. Behm, Encapsulation of Ru nanoparticles: Modifying the reactivity toward CO and CO_2 methanation on highly active Ru/TiO_2 catalysts, Applied Catalysis B-Environmental, 270 (2020) 118846.

[7] A. Faizah, B. Rida, G. Rohama, R. Zohaib Ur, M. Hammad, A. Adnan, S. Muhammad, D. Davoud, A. Ghazanfar, J. Karl, Synthesis and electrochemical investigations of ABPBI grafted montmorillonite based polymer electrolyte membranes for PEMFC applications, Renewable Energy, 164 (2021) 709-728.

[8] W. Tu, Y.H. Chin, Catalytic consequences of chemisorbed oxygen during methanol oxidative dehydrogenation on Pd clusters, Acs Catalysis, 5 (2015) 3375-3386.
[9] W. Tu, Y.H. Chin, Catalytic consequences of the identity and coverages of reactive intermediates during methanol partial oxidation on Pt clusters, Journal of Catalysis, 313 (2014) 55-69.
[10]M. Monai, T. Montini, M. Melchionna, T. Duchon, P. Kus, C. Chen, N. Tsud, L. Nasi, K.C. Prince, K. Veltruska, V. Matolin, M.M. Khader, R.J. Gorte, P. Fornasiero, The effect of sulfur dioxide on the activity of hierarchical Pd-based catalysts in methane combustion, Applied Catalysis B-Environmental, 202 (2017) 72-83.
[11]R.K. Singha, A. Yadav, A. Shukla, M. Kumar, R. Bal, Low temperature dry reforming of methane over Pd-CeO_2 nanocatalyst, Catalysis Communications, 92 (2017) 19-22.